

Quantification and prediction of human fetal (-)- Δ^9 -tetrahydrocannabinol/(\pm)-11-OH- Δ^9 -tetrahydrocannabinol exposure during pregnancy to inform fetal cannabis toxicity

Received: 12 November 2023

Accepted: 2 January 2025

Published online: 18 January 2025

 Check for updates

Aditya R. Kumar¹, Lyndsey S. Benson², Erica M. Wymore³, Jocelyn E. Phipers³, Jennifer C. Dempsey⁴, Lucinda A. Cort⁴ & Jashvant D. Unadkat¹ ✉

Prenatal cannabis use is associated with neurodevelopmental deficits, likely due to exposure to the psychoactive cannabinoid, (-)- Δ^9 -tetrahydrocannabinol, and its active metabolite, (\pm)-11-OH- Δ^9 -tetrahydrocannabinol. To determine causality, preclinical studies mimicking human fetal cannabinoid exposure must be conducted. Here we show cannabinoid concentrations across gestation in maternal plasma and paired fetal tissues in trimester 1 and 2 and maternal plasma and fetal umbilical venous plasma in trimester 3. The mean \pm SD trimester 1 and 2 (-)- Δ^9 -tetrahydrocannabinol fetal brain/maternal plasma is 0.50 ± 0.18 ($n = 3$), 0.45 ± 0.28 ($n = 14$), respectively; trimester 3 (-)- Δ^9 -tetrahydrocannabinol umbilical venous plasma/maternal plasma is 0.35 ± 0.13 ($n = 18$). To predict fetal cannabinoid exposure at different prenatal cannabis doses (oral or inhaled), we used a verified maternal-fetal physiologically based pharmacokinetic model. At an inhalational and oral dose of 10 mg (-)- Δ^9 -tetrahydrocannabinol, the model-predicted average fetal brain steady-state (-)- Δ^9 -tetrahydrocannabinol/(\pm)-11-OH- Δ^9 -tetrahydrocannabinol concentrations, at gestational week 15, are 3.7/7.0 nM and 0.73/8.9 nM, respectively. Our maternal-fetal physiologically based pharmacokinetic model can guide future studies to inform risks associated with prenatal cannabis use.

In the United States, 10–23% of pregnant people consume cannabis^{1,2} raising concerns about the effect of such consumption on the offspring. Retrospective analysis to determine association between neurodevelopmental deficits in the offspring and maternal cannabis use^{3–5} is confounded by factors such as variable frequency and potency of cannabis use, abuse of other drugs, and lack of data on cannabis exposure throughout pregnancy. Despite accounting for some of these confounding factors, prenatal cannabis use appears linked to increased behavioral problems (e.g., inattention, aggression, hyperactivity) and lower cognition (e.g., quantitative scores, verbal

reasoning, IQ)^{5–9} in the offspring. However, all potential confounding factors cannot be accounted for by these retrospective analyses. At the same time, it is unethical to conduct a randomized controlled prospective study to investigate the effects of prenatal cannabis on human neurodevelopment.

To resolve the above dilemma, studies can be conducted in animals with cannabis constituents that are thought to cause the cannabis-related neurodevelopmental deficits. These studies should be conducted at the human relevant observed exposures of these constituents. (-)- Δ^9 -tetrahydrocannabinol (Δ^9 -THC), the main active psychoactive

¹Department of Pharmaceutics, University of Washington School of Pharmacy, Seattle, WA, USA. ²Department of Obstetrics and Gynecology, University of Washington School of Medicine, Seattle, WA, USA. ³Department of Pediatrics, University of Colorado School of Medicine, Aurora, CO, USA. ⁴Department of Pediatrics, University of Washington School of Medicine, Seattle, WA, USA. ✉ e-mail: jash@uw.edu

constituent in cannabis, along with its primary metabolite (\pm)-11-hydroxy- Δ^9 -THC (11-OH-THC), are thought to be constituents causing neurodevelopmental deficits from prenatal cannabis use. While studies where pregnant animals (primarily rodents) were exposed to the cannabis plant or the active constituent (Δ^9 -THC) have been performed^{10,11}, the fetal brain or plasma Δ^9 -THC/11-OH-THC were not measured, making it unclear whether they were conducted at human relevant exposures. For this reason, the primary goals of our study were two-fold. First, to quantify the concentration of Δ^9 -THC and 11-OH-THC in human maternal plasma (MP), placenta, and fetal tissue from the 1st and 2nd trimester (T1 and T2) and in MP, placenta, and umbilical venous plasma (UVP) from the 3rd trimester (T3) of pregnant individuals who had consumed recreational cannabis prior to delivery or termination. These samples provide a single time-point (snapshot) of the fetal cannabinoid concentrations in plasma and various tissues, relative to MP, but are not informative of the time-dependent cannabinoid fetal exposure (i.e., the area under the plasma concentration-time profile). For obvious reasons, such Δ^9 -THC/11-OH-THC exposure cannot be measured *in vivo*. However, such exposure can be predicted using our linked Δ^9 -THC/11-OH-THC maternal-fetal physiologically based pharmacokinetic (m-f-PBPK) model. Therefore, our secondary goal was to populate our current m-f-PBPK model^{12–15} with the various Δ^9 -THC/11-OH-THC maternal-fetal disposition parameters following oral or inhalational cannabis consumption (Supplementary Table 1). Then, we determined if these predicted fetal plasma/tissue concentrations agree with those observed (Fig. 1). An agreement would deem the model to be verified and, therefore, could be used to predict the total and unbound fetal tissue and plasma Δ^9 -THC/11-OH-THC exposure across different gestational ages for different routes, doses and frequency of cannabis consumption. Such predictions will provide critical data for design of *in vitro* and *in vivo* Δ^9 -THC/11-OH-THC neurodevelopmental toxicity studies. Here we show that, throughout gestation, both UVP and fetal brain exposure to Δ^9 -THC was reduced relative to that in the MP; however, such exposure was predicted to be greatest at gestation week (GW) 15. In addition, our m-f-PBPK model was able to predict these exposures.

Results

Enrollment, Dose Consumed and Time of Sampling from Last Consumption

Forty-one participants were enrolled in the T1/T2 study and 40 completed the study (18 T1; 22 T2); a positive urine toxicology test for cannabinoids disqualified one participant. Thirty-four participants were enrolled in the T3 study, 26 completed the study and 8 withdrew (see Supplementary Table 2 for demographics). The gestational age for

the participants was 10 ± 1.1 , 15 ± 1.9 , and 38 ± 1.7 weeks, for T1, T2 and T3, respectively. In the T1 study, 1 reported oral Δ^9 -THC and 17 reported inhalation Δ^9 -THC consumption prior to pregnancy termination; in the T2 study all 22 T2 participants reported inhalation consumption; in the T3 study, 1 reported only oral consumption, 18 reported only inhalation consumption, and 7 reported mixed oral and inhalation consumption.

On the termination day, the T1/T2 study participants self-reported consuming, on average, 1.3 g cannabis plant (inhalation, $n = 27$; Δ^9 -THC dose unknown) or 100 mg (318 μ mol) Δ^9 -THC (oral, $n = 1$). The time between the last consumption of cannabis and the survey was: < 4 h ($n = 10$); 4–12 h ($n = 9$); 12–24 h ($n = 16$); 24–36 h ($n = 3$); 36–48 h ($n = 2$); these were the time bins provided to the participants. On average, there was a 4.74-hour delay between the survey and sample collection.

In the T3 study, prior to delivery, the participants reported consuming, on average, 0.79 g cannabis plant by inhalation ($n = 20$; Δ^9 -THC dose unknown) or 28 mg (89 μ mol) Δ^9 -THC orally ($n = 7$). The time between the last consumption and the survey was: 4–12 h ($n = 1$); 12–24 h ($n = 4$); 24–36 h ($n = 8$); 36–48 h ($n = 2$); 48–72 h ($n = 2$); > 72 h ($n = 9$). On average, there was a 16.1-hour delay between survey and sample collection.

Given that a majority of the above samples were obtained more than 12 h after last consumption, irrespective of GW, not surprisingly, there was no evident association between the cannabinoid UVP/MP or fetal tissue/MP concentration ratio and sampling time since the last dose. This is because distributional equilibrium of Δ^9 -THC and 11-OH-THC between maternal plasma and tissue (including fetal) was expected to be reached by 12 h. For this reason, the concentration data (all normalized to MP concentration), for all routes of Δ^9 -THC consumption and sampling times, were pooled and analyzed as described below.

Observed Fetal UVP/Tissue and Maternal Concentration in Trimester 1, 2, and 3

For T1, T2, and T3 participants, the average placenta concentration across the three sampled regions is reported as they did not differ between the regions. The average paired T1 placenta and T2 placenta, fetal brain, and kidney concentrations of Δ^9 -THC and COOH-THC were significantly lower than the corresponding MP concentration (Fig. 2, Table 1). The average paired T3 placenta and UVP concentrations of Δ^9 -THC and COOH-THC were significantly lower than the corresponding MP concentration (Fig. 2, Table 1). While 11-OH-THC was detectable in several MP samples, it was detectable in only one UVP and one placenta sample (Table 1). T3 MP and UVP as well as T1/T2 MP and fetal tissue

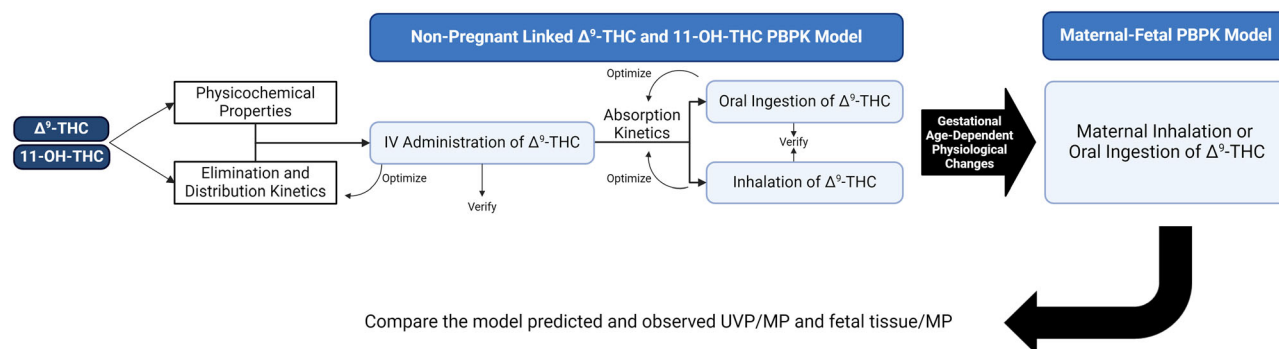


Fig. 1 | Schematic showing Δ^9 -THC and 11-OH-THC PBPK model development and verification for inhalation and oral consumption of Δ^9 -THC by the non-pregnant population followed by extension to the pregnant population (m-f-PBPK model). First, the model was built in Simcyp V22 for the healthy non-pregnant population by optimizing and verifying the Δ^9 -THC elimination and distribution kinetics after intravenous administration. Then, Δ^9 -THC absorption kinetics and 11-OH-THC elimination and distribution kinetics were verified after

inhalation and oral Δ^9 -THC consumption. The Δ^9 -THC kinetics in the non-pregnant model were also verified through drug-drug interaction and pharmacogenetic studies. Then, using our in-house m-f-PBPK model, built in MATLAB Simulink R2023a, which includes the placental and fetal compartments as well as gestational age-dependent physiological changes, the umbilical venous plasma (UVP) and fetal tissue concentrations were predicted. Figure was created with BioRender.com.

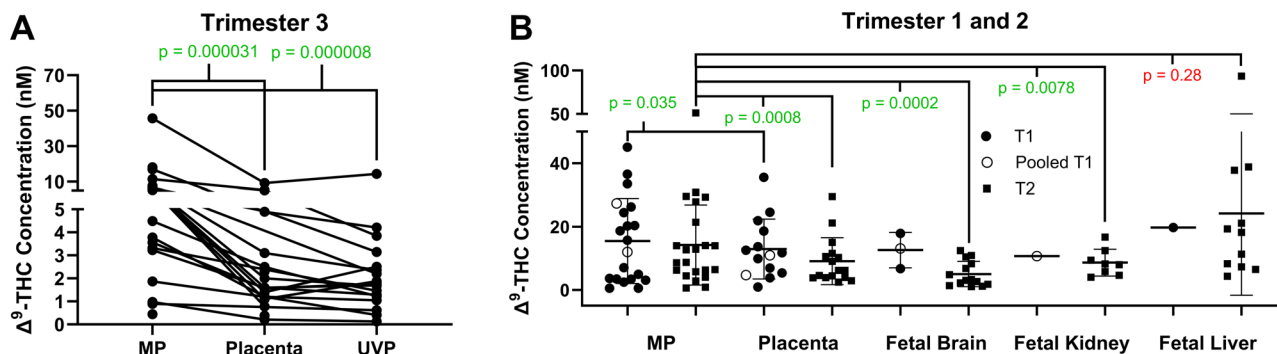


Fig. 2 | Maternal plasma (MP), umbilical venous plasma (UVP), placental and fetal tissue Δ^9 -THC concentrations in trimester 1 (T1), 2 (T2), and 3 (T3) pregnancies. A The T3 UVP ($n = 18$) and placenta ($n = 18$) concentrations within each maternal-fetal dyad were significantly lower than that in the corresponding MP ($n = 21$). **B** The T1 placenta ($n = 12$) and T2 placenta ($n = 16$), fetal brain ($n = 14$), and fetal kidney ($n = 8$) concentrations within each maternal-fetal dyad were

significantly lower than that in the corresponding MP. T2 fetal liver ($n = 11$) concentrations are not significantly different than its corresponding MP. Data are represented as mean \pm SD and the open symbols denote tissues or MP that were pooled ($n = 3$) for analyses due to small volume/size available. All comparisons were made with a two-tailed, Wilcoxon signed rank test. Δ^9 -THC: 1 nM = 0.314 ng/mL. Source data are provided in Supplementary Tables 3–4.

cannabinoid concentrations were highly variable (Supplementary Tables 3–6) likely because of variability in the time since last consumption and in the amount of Δ^9 -THC consumed that resulted in variable MP concentration. This conclusion is reinforced by the observation that the variability is greatly reduced when the fetal tissue or UVP concentration is expressed relative to the corresponding MP (Supplementary Tables 3–6).

Non-pregnant PBPK model optimization and verification

For the non-pregnant (NP) model, the predicted/observed Δ^9 -THC and 11-OH-THC area under the concentration-time curve to time of infinity (AUC_{inf}) and maximum concentration (C_{max}) fell within the acceptance range for all datasets regardless of route of consumption (IV, inhalation, or oral). The same was true for the ratio of the plasma exposure of Δ^9 -THC C_{max} and AUC_{inf} in the presence and absence of drug interaction (cytochrome P450s, CYP2C9 and CYP3A) or CYP2C9 genetic polymorphism (Supplementary Figs. 1–3, Supplementary Table 7).

Comparison of the maternal-fetal PBPK model predicted and observed UVP/MP and fetal tissue/MP values

Our m-f-PBPK model predictions at GW15 and 38 aligned with the observed snapshot T2 fetal brain/MP (0.54), T2 fetal liver/MP (1.8), T2 fetal kidney/MP (0.73), and T3 UVP/MP (0.31) values and were within the acceptance range (Fig. 3, Supplementary Table 8). These verification simulations were conducted following daily maternal Δ^9 -THC inhalation (100 mg; 318 μ mol) at GW15 and 38 to mirror the average gestational age of T2 and T3 participants in our study and the frequency/amount of Δ^9 -THC consumed. Two assumptions were made for these predictions. First, that the snapshot values (observed and predicted) were obtained when distributional equilibrium between tissue and plasma was reached (i.e., > 12 h; see Supplementary Fig. 4). Parenthetically, assuming linear pharmacokinetics, these concentration ratios should be and are independent of the consumed dose and route of consumption. Second, that the Δ^9 -THC fetal-maternal transport was at the basal membrane of the syncytiotrophoblast, mediated by an influx transporter located there. In contrast, all fetal to MP ratios were over-predicted (Supplementary Fig. 4) if Δ^9 -THC transport was assumed to be due to efflux transport at the apical membrane of the syncytiotrophoblast. Therefore, all subsequent m-f-PBPK model predictions were conducted assuming that the observed Δ^9 -THC fetal-maternal intrinsic placental transport ($CL_{int,T}$) was by a basal influx transporter(s).

m-f-PBPK Model Predicted Gestational Age-Dependent Changes in Maternal Δ^9 -THC/11-OH-THC Exposure

After Δ^9 -THC inhalation, the Δ^9 -THC and 11-OH-THC MP average steady-state concentration ($C_{ss,avg}$) decreased marginally as gestational age advanced (Table 2, Fig. 4). After oral Δ^9 -THC consumption, the effect was modestly larger (Table 3, Fig. 4).

m-f-PBPK Model Predicted Gestational Age-Dependent Changes in Fetal Plasma and Brain Δ^9 -THC/11-OH-THC Exposure

GW15 is the earliest GW for which predictions can be made by our m-f-PBPK model. For this reason, we predicted the changes in total and unbound UVP and fetal brain Δ^9 -THC/11-OH-THC at GW 15–40 (Tables 2 and 3, Fig. 5; exposure at GW25 and 38 was in between 15 and 40). After Δ^9 -THC inhalation, the predicted Δ^9 -THC and 11-OH-THC UVP/MP $C_{ss,avg}$ ratio ($C_{ss,avg}R$) decreased from 0.46 to 0.29 and from 1.51 to 0.98, respectively, with an increase in GW from 15 to 40. This trend was reproduced after oral Δ^9 -THC consumption (Table 3). Irrespective of inhalational or oral Δ^9 -THC consumption, with a change in the GW, both Δ^9 -THC and 11-OH-THC fetal brain/MP $C_{ss,avg}R$ changed in parallel with their corresponding UVP/MP $C_{ss,avg}R$ (Tables 2 and 3). This is because the fetal brain tissue to plasma ratio (K_p) was assumed to be constant across gestational age. As expected, the predicted cannabinoid fetal brain/MP and fetal brain/UVP $C_{ss,avg}R$ were independent of the route of consumption. At GW15, after a 10 mg (32 μ mol) daily dose of Δ^9 -THC consumed by inhalation (range: 5–40 mg), the predicted fetal brain Δ^9 -THC and 11-OH-THC $C_{ss,avg}$ were 3.7 nM (1.9–14.8 nM for dose range 5–40 mg) and 7.0 nM (range: 3.5–28.1 nM), respectively (Fig. 6). After daily oral consumption of 10 mg (32 μ mol) Δ^9 -THC (range: 5–40 mg), the predicted fetal brain Δ^9 -THC and 11-OH-THC $C_{ss,avg}$ were lower, 0.73 nM (range: 0.36–2.9) and 8.9 nM (4.4–35 nM), respectively (Fig. 6). The fetal brain $C_{ss,avg,u}$ of these cannabinoids is even lower due to extensive binding to the brain tissue. Therefore, after a daily inhalation dose of 10 mg (32 μ mol) Δ^9 -THC at GW15, the predicted fetal brain $C_{ss,avg,u}$ of Δ^9 -THC and 11-OH-THC were 0.014 nM and 0.014 nM, respectively and after a typical daily oral consumption of 10 mg (32 μ mol) Δ^9 -THC, they were 0.003 nM and 0.017 nM, respectively.

As expected, the predicted cannabinoid $C_{ss,max}$ values for each tissue or UVP were much higher than the $C_{ss,avg}$ values. For example, with an inhalation dose of 10 mg (32 μ mol) Δ^9 -THC at GW15, the predicted UVP $C_{ss,max}$ were 95 nM Δ^9 -THC and 13 nM 11-OH-THC and the corresponding fetal brain $C_{ss,max}$ were 88 nM Δ^9 -THC and 40 nM 11-OH-THC (Fig. 6). Likewise, with a typical oral dose of 10 mg (32 μ mol) Δ^9 -

Table 1 | Trimester 1, 2, and 3 Mean Δ^9 -THC, 11-OH-THC, and COOH-THC Concentrations in the Umbilical Venous Plasma (UVP), Placenta and Fetal Tissues as well as Their Values Relative to the Corresponding Maternal Plasma (MP) Concentration

	Δ^9 -THC			11-OH-THC			COOH-THC		
	Trimester 1	Trimester 2	Trimester 3	Trimester 1	Trimester 2	Trimester 3	Trimester 1	Trimester 2	Trimester 3
Maternal Plasma (nM)	15.0 \pm 13.9 (n = 18) ^a	14.2 \pm 12.7 (n = 17) ^{b,c,d}	7.90 \pm 9.82 (n = 21) ^{d,f}	6.12 \pm 4.38 (n = 13)	5.53 \pm 3.85 (n = 12)	4.81 \pm 7.89 (n = 10)	124 \pm 107 (n = 18) ^g	74.9 \pm 59.7 (n = 18) ^{h,i,j,k}	108 \pm 272 (n = 22) ^{j,m}
Umbilical Venous Plasma (nM)	---	---	2.55 \pm 3.14 (n = 18) ^b	---	---	5.20 (n = 1)	---	---	23.4 \pm 36.9 (n = 19) ^j
UVP/MP	---	---	0.35 \pm 0.13 (n = 18)	---	---	0.20 (n = 1)	---	---	0.36 \pm 0.18 (n = 19)
Fetal Brain (nM)	12.6 \pm 5.60 (n = 3)	5.01 \pm 4.00 (n = 14) ^b	---	BLOQ	13.4 (n = 1)	---	20.6 \pm 5.00 (n = 3)	16.8 \pm 10.3 (n = 9) ^h	---
Fetal Brain/MP	0.50 \pm 0.18 (n = 3)	0.45 \pm 0.28 (n = 14)	---	---	0.29 (n = 1)	---	0.11 \pm 0.03 (n = 3)	0.17 \pm 0.074 (n = 9)	---
Fetal Kidney (nM)	10.7 (n = 1)	8.64 \pm 4.25 (n = 8) ^c	---	5.15 (n = 1)	6.80 \pm 5.51 (n = 6)	---	48.1 (n = 1)	27.4 \pm 28.6 (n = 12) ^j	---
Fetal Kidney/MP	0.89 (n = 1)	0.48 \pm 0.24 (n = 8)	---	1.36 (n = 1)	0.68 \pm 0.56 (n = 6)	---	0.63 (n = 1)	0.23 \pm 0.14 (n = 12)	---
Fetal Liver (nM)	19.7 (n = 1)	24.2 \pm 25.9 (n = 11)	---	BLOQ	14.1 \pm 14.5 (n = 7)	---	66.7 (n = 1)	51.3 \pm 44.4 (n = 12) ^j	---
Fetal Liver/MP	0.75 (n = 1)	1.33 \pm 0.71 (n = 11)	---	---	1.47 \pm 0.99 (n = 6)	---	0.39 (n = 1)	0.44 \pm 0.11 (n = 12)	---
Placenta (nM)	13.8 \pm 9.93 (n = 12) ^a	9.10 \pm 7.45 (n = 16) ^d	2.37 \pm 2.24 (n = 18) ^f	5.21 (n = 2)	BLOQ	27.0 (n = 1)	31.5 \pm 23.9 (n = 11) ^g	31.7 \pm 18.1 (n = 8) ^k	21.2 \pm 31.8 (n = 10) ^m
Placenta/MP	0.96 \pm 1.18 (n = 12)	0.61 \pm 0.29 (n = 16)	0.37 \pm 0.18 (n = 16)	0.66 (n = 2)	---	1.04 (n = 1)	0.22 \pm 0.096 (n = 11)	0.46 \pm 0.63 (n = 8)	0.26 \pm 0.15 (n = 10)

Dat presented as Mean \pm SD, unless n = 1; MP: maternal plasma; UVP: umbilical venous plasma; BLOQ: below limit of quantification; ---: no sample, ratio cannot be calculated; The marked fetal UVP or tissue cannabinoid concentrations were significantly different than the corresponding MP concentration ($p = 0.035^a$; 0.0002^b ; 0.0078^c ; 0.0008^d ; 0.000008^e ; 0.000031^f ; 0.000008^g ; 0.000008^h ; 0.000004^i ; 0.000004^j ; 0.000004^k ; 0.000004^l ; 0.000004^m ; two-tailed, Wilcoxon signed rank test); Δ^9 -THC: 1 nM = 0.314 ng/mL; 11-OH-THC: 1 nM = 0.330 ng/mL; COOH-THC: 1 nM = 0.344 ng/mL.

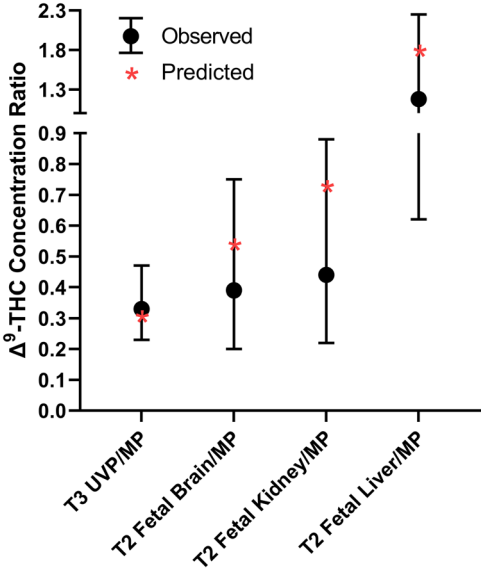


Fig. 3 | m-f-PBPK model snapshot predicted vs. observed steady-state Δ^9 -THC umbilical venous plasma (UVP) and fetal tissue concentration relative to the corresponding maternal plasma (MP) concentration. The m-f-PBPK model predicted (*) trimester 3 (T3; GW38) UVP/MP (n = 18) and trimester 2 (T2; GW15) fetal tissue/MP (fetal brain/MP: n = 14; fetal kidney/MP: n = 8; fetal liver/MP: n = 11) fell within the acceptance range (horizontal lines; filled circles denote the median and bars denote the range of the observed values). The m-f-PBPK model predicted values were those at 12 h post Δ^9 -THC consumption (inhalation or oral) when distributional equilibrium between plasma and tissue Δ^9 -THC concentration was expected to have been reached (see Supplementary Fig. 4). Source data are provided in Supplementary Tables 3–4.

THC, at GW15, the predicted UVP $C_{ss,max}$ were 2.8 nM Δ^9 -THC and 12 nM 11-OH-THC and the corresponding fetal brain $C_{ss,max}$ were 3.9 nM Δ^9 -THC and 38 nM 11-OH-THC (Fig. 6). Theoretically, at any given timepoint the THC and 11-OH-THC fetal brain/UVP should reflect their respective fetal brain K_p . Therefore, they should not change based upon the dosing amount or the route of consumption. However, the absorption rate differs with different routes of consumption causing a difference in the time to reach $C_{ss,max}$ for each route. Thus, the fetal brain/UVP $C_{ss,max}$ is not independent of the route of consumption. Note, the above are the predicted total (not unbound) cannabinoid concentrations. Due to significant tissue or plasma protein binding, the corresponding predicted unbound cannabinoid concentrations were much lower (Tables 2 and 3).

Discussion

We present here quantification of cannabinoid exposure in human UVP or fetal tissues and MP in a large cohort of T1, T2 and T3 pregnant individuals (Table 1). To our knowledge, this is also the first time that a m-f-PBPK model has been applied to predict maternal-fetal cannabinoid exposure after daily consumption of Δ^9 -THC via inhalational or oral route. Our predictions and observations provide insight into how fetal:maternal cannabinoid exposure varies with respect to Δ^9 -THC (or cannabis) dose and route of consumption. In addition, our study provides critical data to inform the design of future in vitro and animal studies to determine the impact of prenatal cannabis use on neuro-developmental toxicity.

Our mean Δ^9 -THC paired UVP/MP observed value at delivery (0.35 ± 0.13 ; n = 18; Table 1) agrees with data from a sparse dataset (n = 3) by Blackard et al. (0.26 ± 0.10)¹⁶. Blackard et al. did not report the concentrations of 11-OH-THC which was quantifiable in only one of our UVP samples (Table 1). Our observed T3 paired mean UVP/MP COOH-THC value (0.36 ± 0.18 ; n = 19; Table 1) was slightly greater than

Table 2 | m-f-PBPK Model Predicted Dose-Normalized Steady-State Total and Unbound Δ^9 -THC and 11-OH-THC Maternal (or Non-pregnant) Plasma, Umbilical Venous Plasma and Fetal Brain Concentrations at 15, 25, and 40 GW of Pregnancy after Daily Inhalation Cannabis Use

Inhalation								
	Δ^9 -THC				11-OH-THC			
	Non-Pregnant	GW15	GW25	GW40	Non-Pregnant	GW15	GW25	GW40
MP or NP $C_{ss,avg}$ (nM/ mg dose)	0.57	0.55	0.50	0.51	0.14	0.14	0.14	0.14
MP or NP $C_{ss,avg,u}$ (nM/ mg dose)	0.0063	0.0060	0.0055	0.0056	0.0017	0.0017	0.0017	0.0016
MP or NP $C_{ss,max}$ (nM/ mg dose)	13.8	13.8	12.8	12.6	1.01	1.00	1.01	0.99
MP or NP $C_{ss,max,u}$ (nM/ mg dose)	0.15	0.15	0.14	0.14	0.012	0.012	0.012	0.012
UVP $C_{ss,avg}$ (nM/mg dose)	NA	0.25	0.16	0.14	NA	0.21	0.17	0.13
UVP/MP $C_{ss,avg}R$	NA	0.46	0.33	0.29	NA	1.51	1.20	0.98
UVP $C_{ss,avg,u}$ (nM/ mg dose)	NA	0.0018	0.0012	0.0010	NA	0.0014	0.0011	0.0009
UVP/MP $C_{ss,avg,u}R$	NA	0.29	0.21	0.18	NA	0.84	0.67	0.55
UVP $C_{ss,max}$ (nM/mg dose)	NA	9.48	3.97	3.70	NA	1.30	0.43	0.33
UVP $C_{ss,max,u}$ (nM/ mg dose)	NA	0.067	0.028	0.026	NA	0.0087	0.0029	0.0022
Fetal Brain $C_{ss,avg}$ (nM/ mg dose)	NA	0.37	0.23	0.18	NA	0.70	0.55	0.43
Fetal Brain/MP $C_{ss,avg}R$	NA	0.68	0.46	0.35	NA	5.08	4.00	3.16
Fetal Brain/UVP $C_{ss,avg}R$	NA	1.50	1.40	1.22	NA	3.36	3.32	3.16
Fetal Brain $C_{ss,avg,u}$ (nM/ mg dose)	NA	0.0014	0.0009	0.0007	NA	0.0014	0.0011	0.0008
Fetal Brain/MP $C_{ss,avg,u}R$	NA	0.24	0.16	0.12	NA	0.81	0.64	0.51
Fetal Brain/UVP $C_{ss,avg,u}R$	NA	0.81	0.76	0.66	NA	0.96	0.95	0.92
Fetal Brain $C_{ss,max}$ (nM/ mg dose)	NA	8.80	1.70	0.81	NA	3.98	1.04	0.63
Fetal Brain $C_{ss,max,u}$ (nM/ mg dose)	NA	0.039	0.0077	0.0033	NA	0.0079	0.0020	0.0012

NA: not applicable; MP: maternal plasma; NP: Non-pregnant plasma; UVP: umbilical venous plasma; $C_{ss,avg}$: average steady-state concentration; $C_{ss,avg,u}$: unbound average steady-state concentration; $C_{ss,max}$: maximum steady-state concentration; $C_{ss,max,u}$: unbound maximum steady-state concentration; $C_{ss,avg}R$: ratio of average steady-state concentration; $C_{ss,avg,u}R$: ratio of unbound average steady-state concentration; Δ^9 -THC: 1 nM = 0.314 ng/mL; 11-OH-THC: 1 nM = 0.330 ng/mL.

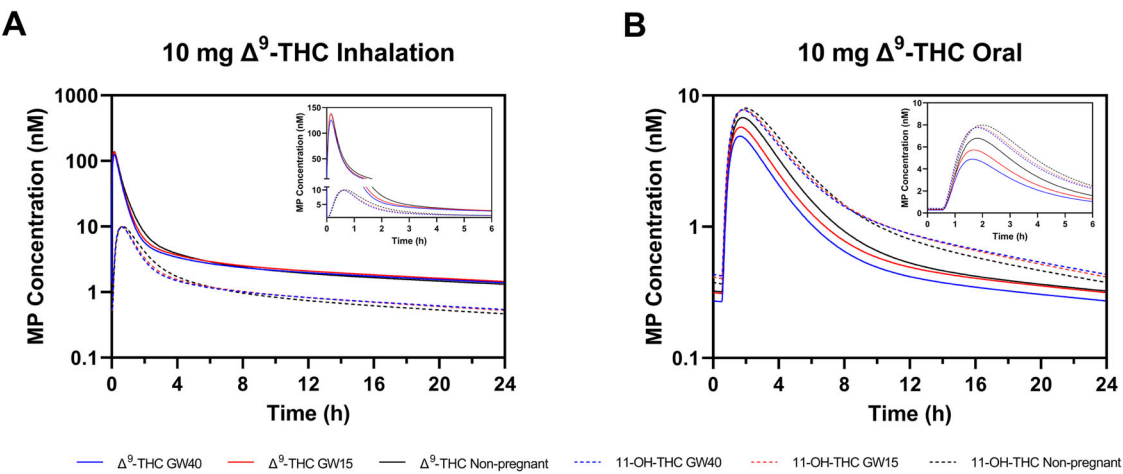


Fig. 4 | m-f-PBPK model predicted non-pregnant and gestational age-dependent Δ^9 -THC/11-OH-THC maternal plasma (MP) concentration-time profiles after daily maternal Δ^9 -THC inhalation (10 mg) or oral (10 mg) consumption. When compared to the non-pregnant population, as gestational week (GW) advanced from 15 to 40, **A** MP Δ^9 -THC $C_{ss,avg}$ and $C_{ss,max}$, after daily Δ^9 -THC (10 mg; 32 μ mol) inhalation, decreased marginally by 4–11% and 0–7%, respectively; **B** MP Δ^9 -THC $C_{ss,avg}$ and $C_{ss,max}$, after daily Δ^9 -THC (10 mg; 32 μ mol) oral consumption, decreased modestly by 15–28% and 16–28%, respectively. Likewise, there was marginal gestational-age dependent decrease (1–5%) in 11-OH-THC MP $C_{ss,avg}$ and $C_{ss,max}$, after both inhalational and oral Δ^9 -THC consumption. Insets show data truncated to 6 h. Δ^9 -THC: 1 nM = 0.314 ng/mL; 11-OH-THC: 1 nM = 0.330 ng/mL. Source data are provided as a Source Data file.

Table 3 | m-f-PBPK Model Predicted Dose-Normalized Steady-State Total and Unbound Δ^9 -THC and 11-OH-THC Maternal (or Non-pregnant) Plasma, Umbilical Venous Plasma and Fetal Brain Concentrations at 15, 25, and 40 GW of Pregnancy after Daily Oral Cannabis Use

Oral	Δ^9 -THC				11-OH-THC			
	Non-Pregnant	GW15	GW25	GW40	Non-Pregnant	GW15	GW25	GW40
MP or NP $C_{ss,avg}$ (nM/mg dose)	0.13	0.11	0.10	0.093	0.18	0.17	0.17	0.17
MP or NP $C_{ss,avg,u}$ (nM/mg dose)	0.0014	0.0012	0.0011	0.0010	0.0021	0.0021	0.0021	0.0021
MP or NP $C_{ss,max}$ (nM/mg dose)	0.68	0.57	0.55	0.49	0.80	0.78	0.78	0.78
MP or NP $C_{ss,max,u}$ (nM/mg dose)	0.0075	0.0063	0.0060	0.0054	0.0096	0.0093	0.0093	0.0093
UVP $C_{ss,avg}$ (nM/mg dose)	NA	0.049	0.034	0.025	NA	0.26	0.21	0.17
UVP/MP $C_{ss,avg}R$	NA	0.44	0.33	0.27	NA	1.51	1.20	0.98
UVP $C_{ss,avg,u}$ (nM/mg dose)	NA	0.0003	0.0002	0.0002	NA	0.0018	0.0014	0.0011
UVP/MP $C_{ss,avg,u}R$	NA	0.28	0.21	0.18	NA	0.84	0.67	0.55
UVP $C_{ss,max}$ (nM/mg dose)	NA	0.28	0.14	0.10	NA	1.16	0.43	0.29
UVP $C_{ss,max,u}$ (nM/mg dose)	NA	0.0020	0.0010	0.0007	NA	0.0077	0.0029	0.0020
Fetal Brain $C_{ss,avg}$ (nM/mg dose)	NA	0.073	0.048	0.031	NA	0.89	0.69	0.54
Fetal Brain/MP $C_{ss,avg}R$	NA	0.66	0.46	0.33	NA	5.08	4.00	3.16
Fetal Brain/UVP $C_{ss,avg}R$	NA	1.50	1.40	1.22	NA	3.36	3.32	3.16
Fetal Brain $C_{ss,avg,u}$ (nM/mg dose)	NA	0.0003	0.0002	0.0001	NA	0.0017	0.0013	0.0010
Fetal Brain/MP $C_{ss,avg,u}R$	NA	0.23	0.16	0.12	NA	0.81	0.64	0.51
Fetal Brain/UVP $C_{ss,avg,u}R$	NA	0.81	0.76	0.66	NA	0.96	0.95	0.92
Fetal Brain $C_{ss,max}$ (nM/mg dose)	NA	0.39	0.15	0.077	NA	3.80	1.35	0.84
Fetal Brain $C_{ss,max,u}$ (nM/mg dose)	NA	0.0015	0.0006	0.0003	NA	0.0074	0.0026	0.0016

NA: not applicable; MP: maternal plasma; NP: Non-pregnant plasma; UVP: umbilical venous plasma; $C_{ss,avg}$: average steady-state concentration; $C_{ss,avg,u}$: unbound average steady-state concentration; $C_{ss,max}$: maximum steady-state concentration; $C_{ss,max,u}$: unbound maximum steady-state concentration; $C_{ss,avg}R$: ratio of average steady-state concentration; $C_{ss,avg,u}R$: ratio of unbound average steady-state concentration; Δ^9 -THC: 1 nM = 0.314 ng/mL; 11-OH-THC: 1 nM = 0.330 ng/mL.

that of Blackard et al. (0.24 ± 0.15 ; $n = 10$)¹⁶. Based on the measured fraction unbound of Δ^9 -THC in adult NP plasma ($f_{u,p} = 0.011$) and in fetal plasma ($f_{u,p,fetus} = 0.0071$), we estimated Δ^9 -THC UVP/MP $C_{ss,avg,u}R$ to be < 0.4 (Supplementary Table 1). The values of Δ^9 -THC fraction unbound (MP $f_{u,p}$ of 0.013, CV = 50%, $n = 18$; $f_{u,p,fetus}$ of 0.0072, CV = 88%, $n = 18$) in our in vivo T3 samples were virtually identical to those listed above. These values were not used in our m-f-PBPK model to keep our predictions prospective, i.e., not dependent on the observed T1/T2/T3 values. Even if the observed values had been used, our predictions would be similar. Collectively, these data suggest that fetal exposure to these cannabinoids (total and unbound) is lower than their corresponding maternal exposure because of influx transport at the basal membrane of the syncytiotrophoblast and fetal liver metabolism. Furthermore, the high degree of plasma protein binding of the cannabinoids will further reduce fetal brain exposure to the unbound cannabinoids provided they are not actively transported into the brain (for further discussion please see below).

The observed Δ^9 -THC fetal brain/MP values in T1 and T2, were 0.50 ± 0.18 and 0.45 ± 0.28 , respectively (Table 1). This similarity for T1 and T2 is not surprising as the mean difference between T1 and T2 gestational age was only 5 weeks (Supplementary Table 2). The human fetal blood-brain barrier (BBB) develops between GW 8–18¹⁷ and the fetal BBB P-glycoprotein protein expression is maximum in the 3rd trimester¹⁸. However, Δ^9 -THC/11-OH-THC and COOH-THC do not appear to be substrates of human P-glycoprotein (P-gp)^{19,20}. Instead, Δ^9 -THC, a lipophilic compound, seems to cross the BBB by

transcellular diffusion. Assuming passive diffusion (and no efflux) of Δ^9 -THC across the BBB, the steady-state unbound fetal brain interstitial fluid:fetal plasma concentration should theoretically be 1.0. Due to the likely significant binding of Δ^9 -THC to fetal brain tissue, the Δ^9 -THC total steady-state fetal brain concentration will be much greater than its corresponding unbound fetal brain concentration. The observed total Δ^9 -THC concentrations in the MP (0.45–51 nM), UVP (0.13–14 nM), and fetal brain (1.0–18 nM), across all gestational ages (Supplementary Tables 3 and 4), and its corresponding unbound concentrations were considerably below those previously tested in vitro (2–15 μ M)^{11,21} and in mouse (dose: 3–5 mg/kg Δ^9 -THC)^{10,11,21} fetal toxicity studies. While the mouse toxicity studies did not measure fetal brain Δ^9 -THC concentrations, we can estimate them because another study measured ~40 nmol/kg (equivalent to nM if brain tissue density is assumed to be 1 g/mL) in fetal brain 2 h after 3 mg/kg Δ^9 -THC was dosed subcutaneously to mice²². Yet another study measured ~460 nmol/kg in fetal brain 15 min after 5 mg/kg was dosed subcutaneously to rats²³.

The cannabinoid UVP/MP and fetal brain/MP values presented above are only snapshots values which are time-dependent and do not represent the steady-state Δ^9 -THC tissue exposure (e.g., $C_{ss,max}$ or $C_{ss,avg}$). Since in vivo measurements of $C_{ss,max}$ or $C_{ss,avg}$ is not possible, prediction by m-f-PBPK modeling is one method to estimate them. This is what we did after our Δ^9 -THC/11-OH-THC PBPK model was verified for the NP population (Supplementary Table 7, Supplementary Figs. 1–3). Since maternal exposure drives fetal exposure to drugs, we first predicted the former.

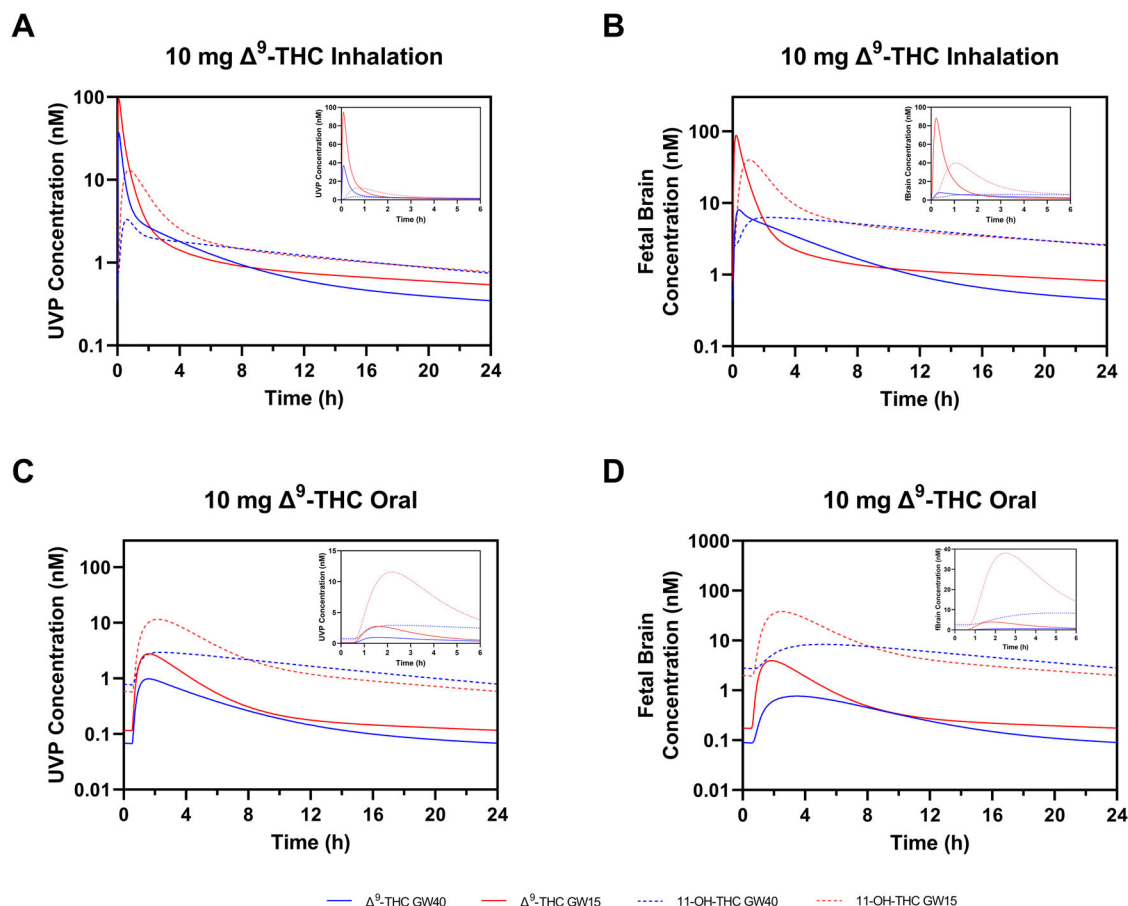


Fig. 5 | m-f-PBPK model predicted gestational age-dependent changes in Δ^9 -THC/11-OH-THC umbilical venous plasma (UVP) and fetal brain concentration-time profiles after daily maternal inhalation (10 mg; 32 μ mol) or oral (10 mg; 32 μ mol) consumption of Δ^9 -THC. The maximum Δ^9 -THC and 11-OH-THC exposure ($C_{ss,avg}$ and $C_{ss,max}$) in the (A, C) UVP and (B, D) fetal brain was predicted to be at the

earliest gestational week (GW15) for which predictions could be made. This was because the predicted maternal plasma (MP), UVP/MP and fetal brain/MP all decreased with increasing gestational age. Insets show data truncated to 6 h. Δ^9 -THC: 1 nM = 0.314 ng/mL; 11-OH-THC: 1 nM = 0.330 ng/mL. Source data are provided as a Source Data file.

When compared with the NP adults, pregnancy and progression in gestational age modestly reduced maternal exposure to Δ^9 -THC. The reduction in the MP $C_{ss,avg}$ was greater after oral Δ^9 -THC (28%) vs. inhalational Δ^9 -THC (11%) consumption (Tables 2 and 3, Fig. 4). This is not surprising as Δ^9 -THC's hepatic clearance (due to its high hepatic extraction) is blood-flow limited. Hepatic blood flow appears not to change during pregnancy^{24,25}. Therefore, its hepatic clearance of Δ^9 -THC is not expected to change after inhalational consumption. In contrast, the Δ^9 -THC MP $C_{ss,avg}$ after oral Δ^9 -THC consumption was affected to a greater extent because Δ^9 -THC's oral clearance is dependent on metabolic clearance rather than hepatic blood flow. And, during pregnancy CYP2C9 is induced, the enzyme primarily responsible for hepatic clearance of Δ^9 -THC^{26,27}. Although hepatic (and not intestinal) CYP3A4 enzyme is induced during pregnancy, it is a significant contributor to only intestinal (but not hepatic) Δ^9 -THC metabolism²⁸. We could not estimate the effect of pregnancy-induced enzyme induction on the maternal exposure of 11-OH-THC because we did not have estimates of the fraction of 11-OH-THC metabolized via various pathways. The above predictions need to be verified when the pharmacokinetics of the cannabinoids are characterized in pregnant people.

Next, we determined if our observed Δ^9 -THC UVP/MP and fetal tissue/MP values were well predicted by our m-f-PBPK model. The predicted values were for sampling times greater than 12 h post-consumption when these values are expected to be relatively constant and when most of our samples were obtained. The values are expected

to be constant because at these times distributional equilibrium between plasma and tissue Δ^9 -THC concentrations should be (and is) achieved (Fig. 3, Supplementary Fig. 4). Each of the predicted T2 fetal tissue/MP values as well as the predicted T3 UVP/MP fell within the acceptance range (Fig. 3). That is, our m-f-PBPK model was successfully verified within the possible time-frame of sampling. The corresponding 11-OH-THC predictions could not be verified because these concentrations could not be quantified in any of the fetal samples except for one UVP and fetal brain sample and only a few fetal liver and kidney samples (Supplementary Table 3 and 5).

As the unbound fetal UVP (and systemic) exposure is determined by the unbound MP Δ^9 -THC exposure, the reduction in fetal (UVP) $C_{ss,avg,u}$ with increasing gestational age reflected the corresponding decrease in MP Δ^9 -THC $C_{ss,avg,u}$ (Tables 2 and 3). At the same time, the predicted ratios (e.g., UVP/MP $C_{ss,avg,u}$) decreased with GW (Table 1) due to the increase in fetal metabolic CL of Δ^9 -THC with GW. Of note, it is important to recognize that the UVP and the fetal circulating Δ^9 -THC concentrations are not the same. As expected, the m-f-PBPK model predicted UVP steady-state concentrations were slightly greater than the corresponding fetal central venous (or arterial) Δ^9 -THC concentrations. This is because the majority (~65%) of UV blood draining the placenta is shunted to the fetal liver¹² (the rest empties into the fetal central vein) where the cannabinoids are metabolized during the first-pass through the fetal liver. This difference between fetal central vein/artery vs UVP concentrations was lesser for 11-OH-THC (only 4–6%), because its first-pass fetal liver metabolism was lesser. Here, for

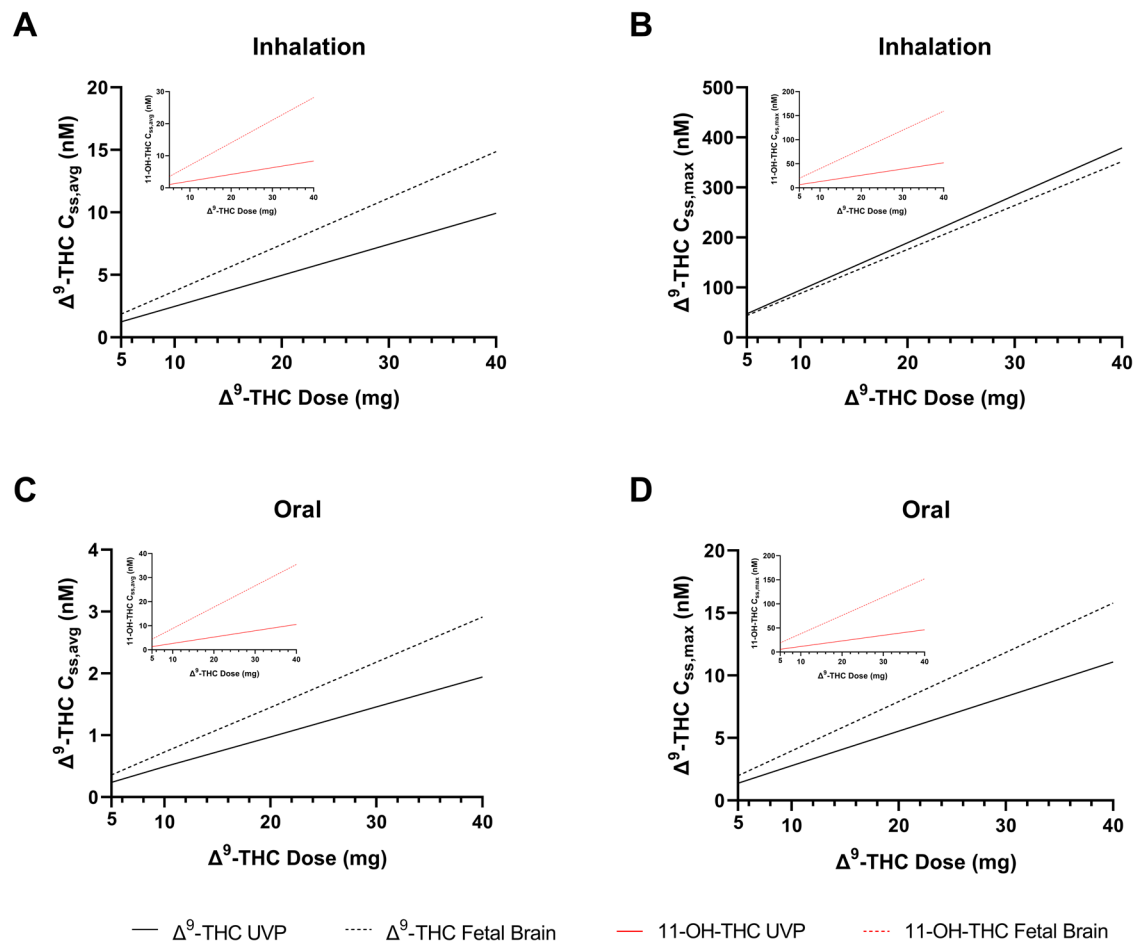


Fig. 6 | m-f-PBPK model predicted dose-dependent average ($C_{ss,avg}$) and maximum ($C_{ss,max}$) steady-state Δ^9 -THC and 11-OH-THC concentration in umbilical venous plasma (UVP) and fetal brain after daily maternal inhalation (10 mg) or oral (10 mg) Δ^9 -THC consumption at gestational week 15. A/B At the inhalation Δ^9 -THC dose (10 mg; 32 μ mol), the predicted UVP $C_{ss,avg}$ & $C_{ss,max}$ were 2.5 & 95 nM Δ^9 -THC and 2.1 & 13 nM 11-OH-THC and for the fetal brain these were 3.7 & 88 nM Δ^9 -

THC and 7.0 & 40 nM 11-OH-THC, respectively. C/D At the typical oral Δ^9 -THC dose (10 mg; 32 μ mol), the predicted UVP $C_{ss,avg}$ & $C_{ss,max}$ were 0.49 & 2.8 nM Δ^9 -THC and 2.6 & 12 nM 11-OH-THC. For the fetal brain these were 0.73 & 3.9 nM Δ^9 -THC and 8.9 & 38 nM 11-OH-THC, respectively. Insets show the 11-OH-THC predicted concentrations. Δ^9 -THC: 1 nM = 0.314 ng/mL; 11-OH-THC: 1 nM = 0.330 ng/mL. Source data are provided as a Source Data file.

simplicity, we have assumed that the different fetal plasma (UVP, central vein, central artery) steady-state concentrations are the same to allow comparison with the observed UVP/MP data. The Δ^9 -THC and 11-OH-THC UVP/MP $C_{ss,avg,uR}$ is determined by the extent of intrinsic placental passive diffusion ($CL_{int,PD}$), intrinsic placental transport clearance ($CL_{int,T}$) and intrinsic fetal hepatic clearance ($CL_{int,fh}$) (Eq. 1).

$$\frac{UVP C_{ss,avg,u}}{MP C_{ss,avg,u}} = \frac{(CL_{int,PD})}{(CL_{int,T} + 2 * CL_{int,fh} + CL_{int,PD})} \quad (1)$$

All these clearance values change with gestational age (Supplementary Table 1). But, as indicated earlier (Supplementary Table 1), the ratio of $CL_{int,PD}$ and $CL_{int,T}$ remained the same. Consequently, the predicted decrease in cannabinoid UVP/MP $C_{ss,avg,uR}$ with GW was due to the increase in fetal liver metabolic CL and not placental transfer CL of the cannabinoids (Tables 2 and 3).

Assuming that both Δ^9 -THC and 11-OH-THC passively diffuse across the fetal BBB, the steady-state unbound fetal brain cannabinoid concentrations should equal the corresponding unbound fetal carotid arterial concentrations. Based on these assumptions, and in agreement with our observed data (Table 1), the predicted fetal brain/UVP $C_{ss,avg,uR}$ or fetal brain/UVP $C_{ss,avg}$ were mostly unchanged by GW (Tables 2 and 3). However, the fetal brain steady-state (total and

unbound) THC concentrations, including the $C_{ss,max}$ were much lower after oral vs. inhalation consumption (i.e., for the same dose). These lower concentrations could potentially result in lower fetal toxicity while still producing the pharmacological effects desired by pregnant people (e.g., alleviation of nausea). The previously observed effects of Δ^9 -THC on neurotoxicity in vitro (at 2 – 15 μ M Δ^9 -THC)^{11,21} may not be observed if re-conducted at the much lower predicted unbound fetal brain concentrations for either 10 mg (32 μ mol) inhalation or oral Δ^9 -THC dose. Of note, accumulation of Δ^9 -THC and 11-OH-THC in the MP, UVP, and fetal brain, at steady-state, for once daily consumption vs. single dose consumption was minimal (<1.07) (Supplementary Fig. 5). From these data, assuming linear pharmacokinetics, the $C_{ss,max}$ and $C_{ss,avg}$ of Δ^9 -THC and 11-OH-THC in the UVP and fetal brain can be computed for any Δ^9 -THC dose (for once-a-day consumption) as they will be proportional to the dose (Fig. 6). Also, our m-f-PBPK model can be used to predict these concentrations for a different frequency of consumption.

Our study has some limitations. First, we did not have definitive information on dose, timing, and frequency of cannabis consumption because our study enrolled pregnant individuals who were already using cannabis (an opportunistic study). Second, we had only a single data point of cannabinoid exposure in each participant. Nevertheless, these single concentration ratio data points were interpretable because, at the times observed, they are/should be independent of the

dose, timing, and frequency of cannabis use. Understandably, the fetal brain concentrations were not verifiable past T2. Though the myelination of fetal neurons may increase as the brain matures, since Δ^9 -THC/11-OH-THC are lipophilic molecules, this will affect their total, but not the unbound brain concentrations; the latter are pharmacologically relevant. Third, our m-f-PBPK model could not be verified for 11-OH-THC, as it was not quantifiable in the majority of in vivo samples. Fourth, we could not predict fetal exposure at < GW15 because we lack physiological data at these GW. When these data are available, such predictions would be important for understanding the impact of cannabis use during a period of rapid brain growth. Lastly, it is possible that constituents of the cannabis plant (e.g., cannabidiol, cannabinol) other than Δ^9 -THC/11-OH-THC or other Δ^9 -THC metabolites (e.g., COOH-THC, 8-OH-THC) contribute to the neurodevelopmental toxicity of cannabis.

In conclusion, we have quantified for the first time Δ^9 -THC, 11-OH-THC, and COOH-THC concentrations in MP, UVP, fetal brain, and placenta tissue in a large cohort of T1, T2 and T3 pregnant people. Moreover, this is the first time a m-f-PBPK Δ^9 -THC model has been employed and verified with respect to fetal tissue exposure to Δ^9 -THC/11-OH-THC after regular cannabis consumption. Our observations and model predictions showed that, throughout gestation, Δ^9 -THC fetal UVP and fetal brain exposure was lower than that in the MP, but, such exposure was greatest at GW15. This lower exposure was due to influx transport at the basal membrane of the syncytiotrophoblast and fetal liver metabolism of Δ^9 -THC. This reduced fetal exposure has the potential to limit neurodevelopmental toxicity from cannabinoid exposure. As randomized clinical trials in pregnant women to determine fetal outcomes are not ethical, future fetal toxicity studies (in vitro or in animals) should be conducted to replicate our predicted unbound fetal UVP and fetal brain Δ^9 -THC/11-OH-THC concentrations at the typical doses consumed by pregnant people. In addition, our m-f-PBPK model could be used to predict fetal exposure for different frequency (and dose) after oral or inhalational consumption of Δ^9 -THC.

Methods

Chemicals and reagents

Ethylenediaminetetraacetic acid (EDTA), d3-11-OH-THC, and d3-COOH-THC were purchased from Sigma-Aldrich (St. Louis, MO). Δ^9 -THC, 11-OH-THC, COOH-THC, and d3- Δ^9 -THC were purchased from Cayman Chemicals (Ann Arbor, MI). Ethyl acetate, hexanes, acetonitrile, sodium phosphate, sucrose, acetic acid (LC-MS/MS grade), formic acid (liquid chromatography-mass spectrometry (LC-MS/MS) grade), LC glass inserts, LC pre-split snap caps, silanized glass culture tubes, and polycarbonate ultracentrifuge tubes were purchased from Fisher Scientific (Hampton, NH).

In vivo study design and procedures

Each study was approved by the respective institutional review board (University of Washington IRB STUDY00008126; Colorado Multiple IRB 19-1757) and performed in accordance with ethical and legal guidelines. Paired fetal and maternal samples were collected from pregnant individuals with known cannabis use. Based on duration of gestation, the samples were divided into two arms. The first arm was a T1 and T2 pregnancy termination study done at the University of Washington while the second was a T3 (term or close to term) delivery study done at the University of Colorado. T1 was defined as up to 11 6/7 GW and T2 was defined as 12 0/7 through 27 6/7 GW, with GW confirmed by a combination of ultrasound and fetal foot length measurement^{29,30}. All collected T2 samples were less than 21 weeks gestation. T3 was defined as > 28 0/7 GW as measured by ultrasound. Informed written consent was obtained from each participant, prior to the study procedures. In addition, all enrolled participants completed a survey on reproductive health history, substance use during pregnancy, and demographics. Regarding the use of cannabis, the collected

information was: 1) route of last use (oral or inhalation); 2) amount consumed during the last use; 3) time since the last use; 4) frequency of use during pregnancy. Participants were compensated \$40 for completing the survey (T1/T2 only) or \$100 for enrollment, the prenatal visit, and the blood draw at delivery (T3 only).

In the T1/T2 termination study, the eligibility criteria were: 1) pregnant individual, 18 years of age or older, seeking termination who had already consented to a termination procedure via dilation and curettage (D&C) or dilation and evacuation (D&E); 2) able to speak and read English; 3) ultrasound-confirmed intrauterine pregnancy; 4) ultrasound dating-determined gestational age of 8–24 weeks; 5) have used, within 48 h of pregnancy termination, Δ^9 -THC-containing cannabis via either oral ingestion or smoking; 6) have not used, during pregnancy, other recreational substances (cocaine, benzodiazepines, opiates, heroin, amphetamines/methamphetamines, or other substances of abuse). A urine toxicology test was administered on the day of the procedure to verify cannabis use and absence of other substance use. Prior to the termination procedure, participants routinely received intravenous (IV) sedatives (e.g., propofol), opioids (e.g., fentanyl), and benzodiazepines (e.g., midazolam). At the time of termination, where possible, maternal blood (5 mL in EDTA tubes), maternal urine, placenta, fetal liver, fetal kidney, and fetal brain tissues were collected. Because of the procedures used for termination, umbilical venous blood could not be collected. MP was separated from blood by centrifugation and immediately stored at 4°C in 1 mL aliquots. MP, placenta and fetal tissues were collected and transported on ice to the University of Washington. Fetal tissues (liver, kidney, and brain) were identified visually and separated within 3 h of collection by an experienced technologist. Placental tissue was divided into 3 specific regions while keeping the villi intact (near umbilical cord, medial, and periphery). Upon identification and separation, the tissues were flash frozen within 1 h of dissection and then immediately stored at –80 °C.

In the T3 delivery study, the eligibility criteria were: 1) pregnant individual, 18–45 years of age; 2) gestational age \geq 16 weeks as determined by last menstrual period and/or early ultrasound; 3) able to speak and read English or Spanish; 4) singleton fetus; 5) current and ongoing use of Δ^9 -THC-containing cannabis; 6) during pregnancy, have not used other recreational drugs (heroin, inhalants, crack, cocaine, alcohol, methamphetamine, hallucinogens, prescription pain relievers, or other drugs of abuse); 7) not positive for coronavirus disease (COVID) at delivery (for safety of study personnel during the pandemic). Per obstetrical clinical policy, verbal screening for prenatal cannabis use was conducted at the first prenatal visit, at 26–28 weeks gestation, and at delivery/hospitalization. Participants, upon disclosure of perinatal cannabis use, were counseled regarding prenatal cannabis use-associated risks and were recommended to decrease or cease cannabis use as part of standardized obstetrical practice. At the delivery time, maternal (5 mL) and umbilical venous blood (3 mL) were simultaneously (or < 30 min of one another) collected in EDTA tubes. The samples were processed and stored identically to the T1/T2 study. Decidua was removed from the placenta tissue and the remaining tissue was divided into 3 specific regions while keeping the villi intact (~10 g each; near umbilical cord, medial, and periphery). Within 1 h of delivery, the tissue was rinsed with saline, flash frozen and stored at –80 °C. Samples were shipped to the University of Washington frozen on dry ice.

Sample processing and bioanalyses

Tissue samples (100–1000 mg) were homogenized with a Bead Ruptor Homogenizer (Omni International, Kennesaw, GA) in buffer (1:4 w/v) containing 10 mM EDTA, 50 mM potassium phosphate buffer (KPi), and 20 mM sucrose. In 20 mL silanized glass culture tubes, 1 mL of tissue homogenate or plasma was spiked in the following order, with 10 μ L of acetonitrile containing 2 μ M internal standard (d3- Δ^9 -THC, d3-11-OH-THC, and d3-COOH-THC), 100 μ L of 1.68% formic acid in water,

and 5 mL of 5:1 hexane:ethyl acetate. The mixture was then agitated vigorously for 30 min on a shaker. Following centrifugation at $200 \times g$ for 10 min at room temperature, the organic supernatant (~5 mL) was transferred to a second silanized glass culture tube and evaporated under nitrogen (40 °C). The residue was reconstituted in 100 μ L acetonitrile and vortexed for 20 seconds. The sample was then transferred to a LC glass insert and stored at -20 °C with a sealed cap until analysis by LC-MS/MS. Fetal and placenta tissue samples were used for sample analyses in their entirety or are being used for further analyses and therefore cannot be made available.

Δ^9 -THC and 11-OH-THC $f_{u,p,fetus}$ was measured in trimester 3 UVP samples, as previously described²⁶. In brief, blank UVP spiked with 500 nM Δ^9 -THC or 11-OH-THC, yielded an $f_{u,p,fetus}$ value of 0.0071 and 0.0067, respectively, as measured by ultracentrifugation (Supplementary Table 1). Similarly, $f_{u,p}$ of these cannabinoids in the T3 UVP and MP was also measured.

Cannabinoid concentrations in plasma and tissue samples were quantified on an Acquity ultra-performance liquid chromatography (UPLC) system (Waters Corporation, Milford, MA) coupled with a Waters Xevo Triple Quadrupole XS in APCI mode (Waters Corporation, Milford, MA). Ten μ L of the processed samples were injected on an Acquity UPLC ethylene bridged hybrid (BEH) C18 column (1.7 μ M 2.1×50 mm) attached to a BEH C18 5 mm guard column (Waters Corporation, Milford, MA) for chromatographic separation. The column was eluted with a mobile phase (0.3 mL/min), consisting of 0.2% acetic acid in acetonitrile and 0.2% acetic acid in water (see Supplementary Table 9 for the gradient conditions). TargetLynx v4.2 (Waters Corporation, Milford, MA) was used to integrate the chromatographic peaks. Blank human plasma and placenta/fetal tissues, spiked at cannabinoid concentrations of 0.05–10 nM, were used as calibrators and processed as per the unknown samples. Quality control samples at 0.1, 1, 10 nM concentrations were within $\pm 20\%$ of the expected values. The lower limit of quantification (LLOQ, defined by a signal to noise ratio > 10), for Δ^9 -THC, 11-OH-THC, COOH-THC in MP, UVP, fetal kidney and fetal brain was 0.05, 0.5, and 0.5 nM, respectively and in placenta and fetal liver was 0.1, 1, and 1 nM, respectively. Samples with concentrations above the highest calibrator concentration were diluted to ensure that they fell within the calibration range.

M-f-PBPK modeling and simulations

In summary, (details listed in Fig. 1), model input values for IV Δ^9 -THC distribution and elimination kinetics in NP adults were first optimized using a training dataset³¹ and then verified (criteria listed below) with two independent datasets^{32,33}. Following this verification, the systemic disposition kinetics of Δ^9 -THC were kept constant and the absorption kinetics were optimized following inhalation and oral consumption using the respective training dataset (Inhalation³¹; Oral³⁴). The absorption kinetics were then verified using independent datasets (Inhalation³⁵; Oral^{36,37}). The fraction of Δ^9 -THC metabolized by each enzyme, determined in vitro (Supplementary Table 1), was confirmed as follows. Δ^9 -THC exposure in individuals with CYP2C9 genetic polymorphism or in the presence of drug-drug interactions (DDIs) was predicted and compared to the observed values (verification criteria listed below)^{38–40}. The verified parameters from these simulations were input into our previously developed m-f-PBPK model⁴¹ (MATLAB Simulink R2023a) refined by Shum et al.¹⁵. This m-f-PBPK model has been developed and verified to predict fetal drug exposure of drugs that cross the placenta passively or by active transport^{12–15}. The model also incorporates gestational age-dependent maternal and fetal physiological parameters^{12,13,42,43} (e.g., magnitude of induction of maternal hepatic CYP enzymes⁴³). This m-f-PBPK model is composed of a full maternal PBPK model with a compartment for each individual organ and a truncated fetal PBPK model with a compartment for each tissue of interest (brain, liver, kidney, intestine) and a lumped compartment that encompasses all the remaining fetal organs. Our MATLAB-based

m-f-PBPK model was utilized in place of Simcyp, as the latter does not have the ability to predict fetal tissue concentrations of metabolites and predicting 11-OH-THC fetal brain exposure was important for this study. To ensure that the models were identical between the two software packages, the NP simulations (initially conducted in Simcyp) were verified in MATLAB. We needed to utilize the Simcyp model for the NP simulations as our MATLAB model was not built to predict DDIs. The population demographics (age, sex distribution, number of participants) and dosing regimen (dose amount, dosing time, route of consumption) for the PBPK model predictions were kept identical to those in the corresponding in vivo study. Unfortunately, we lacked the relevant kinetic data to predict COOH-THC exposure with either the NP or the m-f-PBPK model. However, since COOH-THC is not psychoactive, it is less likely to be involved in fetal neurotoxicity.

Non-pregnant PBPK model. The absorption, distribution and elimination kinetics and physicochemical properties for both Δ^9 -THC and 11-OH-THC were either derived from the literature, estimated by us, or predicted in silico (Supplementary Table 1). $K_{p,tissue}$ was estimated by two different methods: 1) liver, kidney, and brain K_p was optimized to recapitulate the in vivo observed $K_{p,tissue}$ in human postmortem tissue^{44–48}; 2) the Rodgers and Rowland method was used for tissues where postmortem tissue data were not available. We found that Δ^9 -THC exposure, following IV Δ^9 -THC administration only, was sensitive to the K_p of adipose, muscle, and skin and 11-OH-THC exposure was sensitive to the K_p of muscle. Accordingly, these K_p values, for which the cannabinoid concentrations were sensitive, were optimized using the training datasets (listed above) to recapitulate the observed concentration-time profiles following IV Δ^9 -THC dosing. Δ^9 -THC hepatic intrinsic clearance (CL_{int}) was estimated through a middle-out approach⁴⁹ by using the IV training dataset³¹. Briefly, using the dispersion CL model, Δ^9 -THC CL_{int} was back-calculated. Then, the CL_{int} by each CYP isoform was estimated based on the measured fraction metabolized (f_m). If the in vitro Michaelis-Menten constant (K_m)²⁶ was available, the maximum rate of metabolism (V_{max}) was also estimated. The hepatic clearance of 11-OH-THC was estimated using the Δ^9 -THC oral training dataset³⁴ by recapitulating the observed 11-OH-THC AUC_{inf} . For both inhalation and oral consumption of Δ^9 -THC, a first order absorption model was utilized. The rate of absorption (k_a) following inhalation consumption was optimized using the inhalational training dataset³¹ and the fraction absorbed (f_a) was estimated from the in vivo $AUC_{inhalation}/AUC_{IV}$. The f_a following oral consumption was estimated using the in vivo observed $AUC_{inf,fasted}/AUC_{inf,fed}$ with the assumption that f_a would be 1 in the fed state (high-fat diet). The k_a and fraction unbound in the gut ($f_{u,gut}$) were both optimized using the oral Δ^9 -THC training dataset³⁴. All parameter optimization (K_p , k_a , $f_{u,gut}$) was conducted by comparing the predicted vs observed concentrations from the above training datasets using weighted least squares.

M-f-PBPK model. The model⁴¹ was built to predict maternal and fetal exposure to cannabinoids between GW 15–40. Making predictions for T1 fetal exposure $< GW15$ was not possible due to lack of fetal physiological data for those ages. Fetal Δ^9 -THC/11-OH-THC exposure is driven by several factors: 1) their maternal exposure which in turn is driven by their maternal bioavailability and disposition; 2) their extent of distribution across the placenta, determined by their active transport and/or passive diffusion plus placental metabolism; 3) their extent of fetal metabolism (likely by fetal hepatic metabolism). To successfully predict the absolute fetal cannabinoid exposure for a given dose and route of consumption by pregnant individuals, all these disposition parameters need to be estimated (as described below) and incorporated into our m-f-PBPK model.

By conducting Δ^9 -THC/11-OH-THC depletion studies in microsomes derived from human adult liver, intestine, lung, placenta (of different gestational ages), and fetal livers (T2), we have

experimentally determined the metabolic disposition parameters of the cannabinoids. Δ^9 -THC is almost completely metabolized in the adult liver by hepatic CYP2C9 (mostly to 11-OH-THC)²⁶, with some contribution by CYP3A. We assumed that, during the second and third trimesters, hepatic CYP3A was induced 1.99-fold^{28,50}. From in vivo observed steady-state unbound phenytoin (primarily metabolized in the liver via CYP2C9) concentration across GW²⁷, hepatic CYP2C9 induction was estimated to be (1.09, 1.16, 1.29, and 1.31-fold at 15, 25, 38, and 40 GW, respectively). Δ^9 -THC is not metabolized in the placenta but is metabolized in the fetal liver by CYP3A7⁵¹. 11-OH-THC is metabolized in the adult liver by CYP3A, CYP2C9 and uridine 5'-diphosphoglucuronosyltransferases (UGTs) and in the fetal liver by CYP3A7^{26,51}. Although 11-OH-THC is metabolized by the cytosolic alcohol dehydrogenase, aldehyde oxidase and aldehyde dehydrogenase the fraction metabolized via each of these pathways is unknown⁵². $CL_{int, fh}$ was estimated using the product of our previously measured $CL_{int, fh}$ (Δ^9 -THC: 77.1 mL/min/g liver; 11-OH-THC: 11.3 mL/min/g liver)⁵¹ and the fetal liver weight across gestational age (4.98, 33.0, 112, and 129 g at 15, 25, 38, and 40 GW, respectively)¹². Based on previous studies, we made an assumption that CYP3A7 was entirely responsible for the fetal liver metabolism of the cannabinoids⁵¹. CYP3A7 abundance (per gram of liver) does not change with gestational age⁵³.

We have previously quantified that Δ^9 -THC (but not 11-OH-THC) is effluxed in the fetal-maternal direction across the placenta¹⁹. We have shown that this transport is by a transporter(s) other than P-gp or Breast Cancer Resistance Protein (BCRP), efflux transporters that are highly expressed in the human placenta^{54,55}. The location of this unknown transporter(s) could be either on the basal or the apical membrane of the syncytiotrophoblast¹⁹. $CL_{int, PD}$ at term (GW40) was estimated using the previously measured¹⁹, paired, unbound human placental cotyledon clearances ($CL_{u, cotyledon}$) of Δ^9 -THC, 11-OH-THC, and midazolam, along with the in vivo observed midazolam $CL_{int, PD}$ (Eq. 2)

$$CL_{int, PD, THC \text{ or } 11-OH-THC} = \frac{CL_{u, cotyledon, THC \text{ or } 11-OH-THC}}{CL_{u, cotyledon, midazolam}} * CL_{int, PD, midazolam} \quad (2)$$

where midazolam $CL_{int, PD}$ is 500 L/h¹³ and $CL_{u, cotyledon, 11-OH-THC} / CL_{u, cotyledon, midazolam}$ is 0.397, yielding a $CL_{int, PD, 11-OH-THC}$ of 199 L/h (Supplementary Table 1). When Δ^9 -THC placental transport was attributed to efflux at the apical membrane of the syncytiotrophoblast (apical efflux transport) the Δ^9 -THC UVP (at GW38) and fetal tissue (at GW15) exposure was overpredicted (Supplementary Fig. 4). However, the T3 (GW38) UVP/MP and T2 (GW15) fetal tissue/MP concentrations were well-recapitulated when Δ^9 -THC transport was attributed to an influx transporter at the basal membrane of the syncytiotrophoblast (Supplementary Fig. 4). Therefore, we assumed that the observed placenta transport of Δ^9 -THC was due to basal influx transporter(s). Hence, Eq. 2 yielded $CL_{int, PD, THC}$ of 247 L/h (Supplementary Table 1). Passive diffusion of Δ^9 -THC was scaled to earlier gestation based on change in placental weight with GW (assuming that surface area for diffusion changes in proportion with placental weight).

Term (GW40) Δ^9 -THC $CL_{int, T}$ was estimated using the previously calculated fraction transported (f_t) from placental perfusion data¹⁹. The estimated $CL_{int, T, THC}$ was 420 L/h based on a projected f_t by basal influx transporter(s) of 0.63 (Supplementary Table 1). We assumed that at earlier GW, the abundance of this unknown Δ^9 -THC transporter also changed in proportion to placental weight (i.e., the Δ^9 -THC f_t remained the same at all GW).

Using our m-f-PBPK model, populated with the above Δ^9 -THC/11-OH-THC parameters, we predicted Δ^9 -THC/11-OH-THC concentrations in MP, UVP, fetal liver, fetal kidney, and fetal brain at GW 15, 25, 38, and 40 weeks. Predictions were made following once daily cannabis use since 95% of T2 participants reported cannabis

use at least once per day and 77% of T3 participants reported cannabis use at least every other day. For these simulations, an inhalation and oral dose of 10 mg Δ^9 -THC was chosen based on a common consumer dose. While the average inhalation dose reported by the in vivo study participants was ~1 gram of cannabis plant (see below; ~100 mg Δ^9 -THC assuming 10% Δ^9 -THC), due to the design of the study, verification was not possible of actual product content, combusted weight, number of puffs, frequency, or time over which the cannabis was consumed. Since this 100 mg dose is higher than what is typically used, we chose a lower average dose and dose-range for simulations (10 mg, dose range 5–40 mg) for both inhalation and oral Δ^9 -THC consumption. We also computed the dose-normalized values for extrapolation to other doses.

The product of measured unbound fractions (in NP plasma as well as an independent set of UVP; Supplementary Table 1) and the predicted total concentrations in MP and UVP was used to calculate unbound concentrations. The f_{up} of the cannabinoids was assumed to be constant across gestational age. We made the assumption that unbound fetal brain concentrations were equivalent to unbound fetal carotid artery concentrations (see discussion above). We could not predict placenta concentrations as we did not have an accurate estimate (predicted or measured) of the fraction of cannabinoids unbound in the placenta tissue ($f_{u, placenta}$) as this fraction, when measured, can be confounded by the significant amount (unknown) of blood contained within the placenta.

Model verification. Predictions from the model were evaluated by comparing the predicted drug exposure with the observed in vivo data (NP: AUC_{inf} and C_{max} ; pregnancy: UVP/MP and fetal tissue/MP concentration ratios at steady-state). If the predicted exposure was within the 99.998% geometric confidence interval (determined based on variability)⁵⁶ of the observed exposure value, the model was considered verified. The interstudy variability¹⁵ across three independent studies was used for verification of the NP model following IV and oral dosing (IV^{31–33} Oral^{34,36,37}). Since inter-study variability is impossible to compute from just two data sets, for verification of the NP model following inhalation dosing, we used the interindividual variability from the most data-rich study³¹. The interindividual variability observed within our in vivo data was also used for verification of the m-f-PBPK model. The observed T1 and T2 fetal tissue concentrations included the cannabinoids contained in the residual blood within the tissues, however the corresponding m-f-PBPK model predicted these concentrations that are devoid of blood. Thus, using the previously estimated residual blood volume contained within these tissues in neonates [i.e., brain (4.0%), kidney (8.5%), and liver (30%)⁵⁷; values for fetus are not available] we added the predicted blood concentrations to the predicted fetal tissue concentrations for comparison of the predicted and observed fetal tissue/MP values. The acceptance range of the Δ^9 -THC AUC_{infR} and C_{maxR} , with and without the DDI or genetic polymorphism was determined based on the magnitude of the effect^{38–40} and the in vivo observed intraindividual variability^{37,58}. The observed NP concentration-time profiles were obtained by digitization using the WebPlotDigitizer (version 4.6, <https://apps.automeris.io/wpd/>) or the published individual concentration-time data. For the in vivo data, all AUC_{inf} calculations were estimated using Phoenix Win-Nonlin version 8.3.4.

Statistical analysis

For T1, T2, and T3 studies, a pairwise comparison of MP to UVP, placenta, and fetal tissue for each participant was conducted using the two-tailed, Wilcoxon signed rank test with $p < 0.05$ as statistically significant. All statistical tests were conducted in GraphPad Prism version 8.0.2.

Reporting summary

Further information on research design is available in the Nature Portfolio Reporting Summary linked to this article.

Data availability

All data generated or analyzed during this study are included in this published article, its supplementary information, and source data files. All tissue samples were either used in their entirety for sample analysis or are being used for further analyses and therefore cannot be made available. Source data are provided with this paper.

Code availability

The code used for the MATLAB m-f-PBPK model has been deposited at <https://doi.org/10.5281/zenodo.14027760>⁴¹. The model equations for maternal-fetal transfer and fetal disposition have been previously published¹².

References

- Howard, D. S., Dhanraj, D. N., Devaiah, C. G. & Lambers, D. S. Cannabis use based on urine drug screens in pregnancy and its association with infant birth weight. *J. Addict. Med.* **13**, 436–441 (2019).
- Volkow, N. D., Han, B., Compton, W. M. & McCance-Katz, E. F. Self-reported medical and nonmedical cannabis use among pregnant women in the United States. *JAMA* **322**, 167–169, (2019).
- Marchand, G. et al. Birth outcomes of neonates exposed to marijuana in utero: a systematic review and meta-analysis. *JAMA Netw. Open* **5**, e2145653 (2022).
- El Marroun, H. et al. Intrauterine cannabis exposure affects fetal growth trajectories: the generation R study. *J. Am. Acad. Child Adolesc. Psychiatry* **48**, 1173–1181 (2009).
- Paul, S. E. et al. Associations between prenatal cannabis exposure and childhood outcomes: results from the ABCD Study. *JAMA Psychiatry*, <https://doi.org/10.1001/jamapsychiatry.2020.2902> (2020).
- Day, N. L. et al. Effect of prenatal marijuana exposure on the cognitive development of offspring at age three. *Neurotoxicol. Teratol.* **16**, 169–175 (1994).
- Goldschmidt, L., Day, N. L. & Richardson, G. A. Effects of prenatal marijuana exposure on child behavior problems at age 10. *Neurotoxicol. Teratol.* **22**, 325–336 (2000).
- Goldschmidt, L., Richardson, G. A., Willford, J. & Day, N. L. Prenatal marijuana exposure and intelligence test performance at age 6. *J. Am. Acad. Child Adolesc. Psychiatry* **47**, 254–263 (2008).
- Goldschmidt, L., Richardson, G. A., Willford, J. A., Severtson, S. G. & Day, N. L. School achievement in 14-year-old youths prenatally exposed to marijuana. *Neurotoxicol. Teratol.* **34**, 161–167 (2012).
- de Salas-Quiroga, A. et al. Prenatal exposure to cannabinoids evokes long-lasting functional alterations by targeting CB1 receptors on developing cortical neurons. *Proc. Natl. Acad. Sci. USA* **112**, 13693–13698 (2015).
- Peng, H. et al. Effects of prenatal exposure to THC on hippocampal neural development in offspring. *Toxicol. Lett.* **374**, 48–56 (2023).
- Zhang, Z. et al. Development of a novel maternal-fetal physiologically based pharmacokinetic model i: insights into factors that determine fetal drug exposure through simulations and sensitivity analyses. *Drug Metab. Dispos.* **45**, 920–938 (2017).
- Zhang, Z. & Unadkat, J. D. Development of a novel maternal-fetal physiologically based pharmacokinetic model II: verification of the model for passive placental permeability drugs. *Drug Metab. Dispos.* **45**, 939–946 (2017).
- Anoshchenko, O., Storelli, F. & Unadkat, J. D. Successful prediction of human fetal exposure to P-glycoprotein substrate drugs using the proteomics-informed relative expression factor approach and PBPK modeling and simulation. *Drug Metab. Dispos.* **49**, 919–928 (2021).
- Shum, S., Shen, D. D. & Isoherranen, N. Predicting maternal-fetal disposition of fentanyl following intravenous and epidural administration using physiologically based pharmacokinetic modeling. *Drug Metab. Dispos.* **49**, 1003–1015 (2021).
- Blackard, C. & Tennes, K. Human placental transfer of cannabinoids. *N. Engl. J. Med.* **311**, 797 (1984).
- Goasdoue, K., Miller, S. M., Colditz, P. B. & Bjorkman, S. T. Review: the blood-brain barrier; protecting the developing fetal brain. *Placenta* **54**, 111–116 (2017).
- Daood, M., Tsai, C., Ahdab-Barmada, M. & Watchko, J. F. ABC transporter (P-gp/ABCB1, MRP1/ABCC1, BCRP/ABCG2) expression in the developing human CNS. *Neuropediatrics* **39**, 211–218 (2008).
- Kumar, A. R. et al. Understanding the mechanism and extent of transplacental transfer of (-)-Δ(9)-tetrahydrocannabinol (THC) in the perfused human placenta to predict in vivo fetal THC Exposure. *Clin. Pharm. Ther.* **114**, 446–458 (2023).
- Chen, X., Unadkat, J. D. & Mao, Q. Tetrahydrocannabinol and its major metabolites are not (or are poor) substrates or inhibitors of human P-glycoprotein [ATP-binding cassette (ABC) B1] and breast cancer resistance protein (ABCG2). *Drug Metab. Dispos.* **49**, 910–918 (2021).
- Tortoriello, G. et al. Miswiring the brain: delta9-tetrahydrocannabinol disrupts cortical development by inducing an SCG10/stathmin-2 degradation pathway. *EMBO J.* **33**, 668–685 (2014).
- Maciel, I. S. et al. Perinatal CBD or THC exposure results in lasting resistance to fluoxetine in the forced swim test: reversal by fatty acid amide hydrolase inhibition. *Cannabis Cannabinoid Res.* **7**, 318–327 (2022).
- Baglot, S. L. et al. Maternal-fetal transmission of delta-9-tetrahydrocannabinol (THC) and its metabolites following inhalation and injection exposure during pregnancy in rats. *J. Neurosci. Res.* **100**, 713–730 (2022).
- Robson, S. C., Mutch, E., Boys, R. J. & Woodhouse, K. W. Apparent liver blood flow during pregnancy: a serial study using indocyanine green clearance. *Br. J. Obstet. Gynaecol.* **97**, 720–724 (1990).
- Munnell, E. W. & Taylor, H. C. Liver blood flow in pregnancy-hepatic vein catheterization. *J. Clin. Invest.* **26**, 952–956 (1947).
- Patilea-Vrana, G. I. & Unadkat, J. D. Quantifying hepatic enzyme kinetics of (-)-(9)-Tetrahydrocannabinol (THC) and its psychoactive metabolite, 11-OH-THC, through in vitro modeling. *Drug Metab. Dispos.* **47**, 743–752 (2019).
- Tomson, T., Lindbom, U., Ekqvist, B. & Sundqvist, A. Disposition of carbamazepine and phenytoin in pregnancy. *Epilepsia* **35**, 131–135 (1994).
- Zhang, Z., Farooq, M., Prasad, B., Grepper, S. & Unadkat, J. D. Prediction of gestational age-dependent induction of in vivo hepatic CYP3A activity based on HepaRG cells and human hepatocytes. *Drug Metab. Dispos.* **43**, 836–842 (2015).
- FitzSimmons, J., Fantel, A. & Shepard, T. H. Growth parameters in mid-trimester fetal Turner syndrome. *Early Hum. Dev.* **38**, 121–129 (1994).
- Shepard, T. H. Growth and development of the human embryo and fetus. In *Endocrine and Genetic Diseases of Childhood* (ed. Gardner, L. I.) pp. 2–3 (W. B. Saunders, Philadelphia, PA, 1969).
- Ohlsson, A. et al. Single dose kinetics of deuterium labelled delta 1-tetrahydrocannabinol in heavy and light cannabis users. *Biomed. Mass Spectrom.* **9**, 6–10 (1982).
- Hunt, C. A. & Jones, R. T. Tolerance and disposition of tetrahydrocannabinol in man. *J. Pharm. Exp. Ther.* **215**, 35–44 (1980).
- Naef, M., Russmann, S., Petersen-Felix, S. & Brenneisen, R. Development and pharmacokinetic characterization of pulmonary and intravenous delta-9-tetrahydrocannabinol (THC) in humans. *J. Pharm. Sci.* **93**, 1176–1184 (2004).
- Oh, D. A., Parikh, N., Khurana, V., Cognata Smith, C. & Vetticaden, S. Effect of food on the pharmacokinetics of dronabinol oral solution

- versus dronabinol capsules in healthy volunteers. *Clin. Pharm.* **9**, 9–17 (2017).
35. McBurney, L. J., Bobbie, B. A. & Sepp, L. A. GC/MS and EMIT analyses for delta 9-tetrahydrocannabinol metabolites in plasma and urine of human subjects. *J. Anal. Toxicol.* **10**, 56–64 (1986).
 36. Lunn, S. et al. Human pharmacokinetic parameters of orally administered delta(9)-tetrahydrocannabinol capsules are altered by fed versus fasted conditions and sex differences. *Cannabis Cannabinoid Res* **4**, 255–264 (2019).
 37. Parikh, N., Kramer, W. G., Khurana, V., Cognata Smith, C. & Veticaden, S. Bioavailability study of dronabinol oral solution versus dronabinol capsules in healthy volunteers. *Clin. Pharm.* **8**, 155–162 (2016).
 38. Stott, C., White, L., Wright, S., Wilbraham, D. & Guy, G. A Phase I, open-label, randomized, crossover study in three parallel groups to evaluate the effect of Rifampicin, Ketoconazole, and Omeprazole on the pharmacokinetics of THC/CBD oromucosal spray in healthy volunteers. *Springerplus* **2**, 236 (2013).
 39. Sachse-Seeboth, C. et al. Interindividual variation in the pharmacokinetics of Delta9-tetrahydrocannabinol as related to genetic polymorphisms in CYP2C9. *Clin. Pharm. Ther.* **85**, 273–276 (2009).
 40. Pharmaceuticals, G. Sativex Oromucosal Spray: Summary of Product Characteristics. (2022).
 41. Kumar, A. R. Delta-9-Tetrahydrocannabinol (THC) and 11-Hydroxy-THC (11-OH-THC) Maternal-Fetal Physiologically Based Pharmacokinetic (PBPK) Model. <https://doi.org/10.5281/zenodo.14027760> (2024).
 42. Abduljalil, K., Pan, X., Clayton, R., Johnson, T. N. & Jamei, M. Fetal Physiologically Based Pharmacokinetic Models: Systems Information on Fetal Cardiac Output and Its Distribution to Different Organs during Development. *Clin. Pharmacokinet.* **60**, 741–757 (2021).
 43. Abduljalil, K., Furness, P., Johnson, T. N., Rostami-Hodjegan, A. & Soltani, H. Anatomical, physiological and metabolic changes with gestational age during normal pregnancy: a database for parameters required in physiologically based pharmacokinetic modeling. *Clin. Pharmacokinet.* **51**, 365–396 (2012).
 44. Mura, P., Kintz, P., Dumestre, V., Raul, S. & Hauet, T. THC can be detected in brain while absent in blood. *J. Anal. Toxicol.* **29**, 842–843 (2005).
 45. Kemp, P. M., Cardona, P. S., Chaturvedi, A. K. & Soper, J. W. Distribution of $\Delta(9)$ -tetrahydrocannabinol and 11-Nor-9-Carboxy- $\Delta(9)$ -tetrahydrocannabinol acid in postmortem biological fluids and tissues from pilots fatally injured in aviation accidents. *J. Forensic Sci.* **60**, 942–949 (2015).
 46. Saenz, S. R., Lewis, R. J., Angier, M. K. & Wagner, J. R. Postmortem fluid and tissue concentrations of THC, 11-OH-THC and THC-COOH. *J. Anal. Toxicol.* **41**, 508–516 (2017).
 47. Withey, S. L., Bergman, J., Huestis, M. A., George, S. R. & Madras, B. K. THC and CBD blood and brain concentrations following daily administration to adolescent primates. *Drug Alcohol Depend.* **213**, 108129 (2020).
 48. Cliburn, K. D., Huestis, M. A., Wagner, J. R. & Kemp, P. M. Cannabinoid distribution in fatally-injured pilots' postmortem fluids and tissues. *Forensic Sci. Int.* **329**, 111075 (2021).
 49. Bansal, S., Ladumor, M. K., Paine, M. F. & Unadkat, J. D. A physiologically-based pharmacokinetic model for cannabidiol in healthy adults, hepatically-impaired adults, and children. *Drug Metab. Dispos.* **51**, 743–752 (2023).
 50. Hebert, M. F. et al. Effects of pregnancy on CYP3A and P-glycoprotein activities as measured by disposition of midazolam and digoxin: a University of Washington specialized center of research study. *Clin. Pharm. Ther.* **84**, 248–253 (2008).
 51. Kumar, A. R., Patilea-Vrana, G. I., Anoshchenko, O. & Unadkat, J. D. Characterizing and quantifying extrahepatic metabolism of (-)-delta(9)-tetrahydrocannabinol (THC) and its psychoactive metabolite, (+/-)-11-hydroxy-delta(9)-THC (11-OH-THC). *Drug Metab. Dispos.* **50**, 734–740 (2022).
 52. Beers, J. L., Authement, A. K., Isoherranen, N. & Jackson, K. D. Cytosolic enzymes generate cannabinoid metabolites 7-carboxycannabidiol and 11-Nor-9-carboxytetrahydrocannabinol. *ACS Med Chem. Lett.* **14**, 614–620 (2023).
 53. Leeder, J. S. et al. Variability of CYP3A7 expression in human fetal liver. *J. Pharm. Exp. Ther.* **314**, 626–635 (2005).
 54. Anoshchenko, O. et al. Gestational age-dependent abundance of human placental transporters as determined by quantitative targeted proteomics. *Drug Metab. Dispos.* **48**, 735–741 (2020).
 55. Mathias, A. A., Hitti, J. & Unadkat, J. D. P-glycoprotein and breast cancer resistance protein expression in human placentae of various gestational ages. *Am. J. Physiol. Regul. Integr. Comp. Physiol.* **289**, R963–969 (2005).
 56. Abduljalil, K., Cain, T., Humphries, H. & Rostami-Hodjegan, A. Deciding on success criteria for predictability of pharmacokinetic parameters from in vitro studies: an analysis based on in vivo observations. *Drug Metab. Dispos.* **42**, 1478–1484 (2014).
 57. Wayson, M. B. et al. Suggested reference values for regional blood volumes in children and adolescents. *Phys. Med Biol.* **63**, 155022 (2018).
 58. Guest, E. J., Aarons, L., Houston, J. B., Rostami-Hodjegan, A. & Galetin, A. Critique of the two-fold measure of prediction success for ratios: application for the assessment of drug-drug interactions. *Drug Metab. Dispos.* **39**, 170–173 (2011).

Acknowledgements

This work was supported by National Institutes of Health [Grant P01 DA032507, J.D.U.; Grants T32 GM007750 and TL1 TR002318, ARK; Grant R24HD000836, IAG listed below]. We would like to thank Dale Whittington for his contribution in optimizing the bioanalysis methodology, Ian A. Glass, Kimberly A. Aldinger, Dan Doherty, Ian G. Phelps, and Yasmeen Otaibi for their contribution in fetal tissue collection, and Ken Mackie (Indiana University) and William J. Jusko (University at Buffalo) for their critical review of the manuscript. Figure 1 was created with BioRender.com.

Author contributions

A.R.K., L.S.B., E.M.W., and J.D.U. designed the research; J.E.P., J.C.D., and L.A.C. collected samples; A.R.K. analyzed samples; A.R.K. developed the model and conducted simulations; A.R.K. and J.D.U. wrote the manuscript.

Competing interests

The work presented in this paper constituted part of the doctoral dissertation for A.R.K. and has been reproduced there. The remaining authors declare no competing interests.

Additional information

Supplementary information The online version contains supplementary material available at <https://doi.org/10.1038/s41467-025-55863-5>.

Correspondence and requests for materials should be addressed to Jashvant D. Unadkat.

Peer review information *Nature Communications* thanks Javier Fernandez-Ruiz, and the other, anonymous, reviewer(s) for their contribution to the peer review of this work. A peer review file is available.

Reprints and permissions information is available at <http://www.nature.com/reprints>

Publisher's note Springer Nature remains neutral with regard to jurisdictional claims in published maps and institutional affiliations.

Open Access This article is licensed under a Creative Commons Attribution-NonCommercial-NoDerivatives 4.0 International License, which permits any non-commercial use, sharing, distribution and reproduction in any medium or format, as long as you give appropriate credit to the original author(s) and the source, provide a link to the Creative Commons licence, and indicate if you modified the licensed material. You do not have permission under this licence to share adapted material derived from this article or parts of it. The images or other third party material in this article are included in the article's Creative Commons licence, unless indicated otherwise in a credit line to the material. If material is not included in the article's Creative Commons licence and your intended use is not permitted by statutory regulation or exceeds the permitted use, you will need to obtain permission directly from the copyright holder. To view a copy of this licence, visit <http://creativecommons.org/licenses/by-nc-nd/4.0/>.

© The Author(s) 2025